River Flow 2014 – Schleiss et al. (Eds)
© 2014 Taylor & Francis Group, London, ISBN 978-1-138-02674-2

New computation method for flood flows and bed variations in a low-lying river with complex river systems

K. Tabata
Chuo University, Tokyo, Japan

S. Fukuoka
Research and Development Initiative, Chuo University, Tokyo, Japan

ABSTRACT: The lower Shinanogawa River is known as a typical low-lying river in Japan. This river system is comprised of several tributaries, a branched river and a no embankment area. In the record-breaking flood observed in 2011, backward flows around confluences and large inundation from the no embankment area were caused due to large inflows from main tributaries. Flood flows and bed variations in such a complex river system have not been studied so far. In this study, we developed a numerical model applying the Bottom Velocity Computation (BVC) method and 2D bed-variation analysis using observed water surface profiles in the lower Shinanogawa River. Finally the mechanisms of the complex flows around river confluences and functions of the flood flow storage in the complex river system were clarified by using the numerical model developed.

1 INTRODUCTION

The lower Shinanogawa River has a complex river system, which is comprised of several tributaries, branched rivers and a no embankment area (see Fig. 1). The Ikarashigawa River and Kariyatagawa River are main tributaries of the lower Shinanogawa River. The Nakanokuchigawa River and the Sekiya diversion Channel bifurcate from the Shinanogawa River at the Nakanokuchigawa Sluice Gate and Shinanogawa Sluice Gate, respectively and the Nakanokuchigawa River joins again at the downstream of the lower Shinanogawa River. No embankment area is located at just upstream of the inflow point of the Kariyatagawa River. In the record-breaking flood observed in 2011, large floods from the Ikarashigawa River and Kariyatagawa River caused a complex flood flow and large inundation in the no embankment area. Flood flows and bed variations in such a complex river system have not been clarified in spite of occurrence of frequent flood disasters.

In the lower Shinanogawa River having the confluences of several tributaries and large longitudinal changes of plan forms and cross-sections, multi-scale flows are developed. They influence each other and generate the complex flood propagation and bed variation. Therefore, it is necessary to establish a numerical model elucidating the small and large scale hydraulic phenomena and bed variations in the whole reach from the river mouth to the Arai weir.

While simulations of complex flows have been made possible by recent advanced 3D turbulence models (Huang et al. 2002; Wu 2008), applications of the 3D model are still limited to small scale phenomena in experimental channels because of large computational load. Therefore, some kind of depth integrated simulation method should be applied to

Figure 1. Plan form of the lower Shinanogawa River and water level observation points.

complex river fields. The depth integrated model taking into a helical flow in a curved channel (Nishimoto 1992) using well developed secondary flow model (Engelund 1974) has proposed. A number of Quasi-3D models taking into vertical distribution of horizontal velocities have been proposed (Ishikawa 1989, Jin 1993). In these models, a vertical distribution of horizontal velocities is solved by 3D momentum equations using a weighted residual method. In recent years, Uchida and Fukuoka (2011; 2012) developed the Bottom Velocity Computation (BVC) method. The BVC method is an integrated multi-scale simulation of flows and bed variations in rivers, which is capable of evaluating vertical distribution of horizontal velocities and bottom velocities by introducing depth-averaged horizontal vorticity equations and horizontal momentum equations on water surface to shallow water equations.

Fukuoka (2011) proposed the numerical method for flood flows and bed variations using time series of observed water surface profiles during a flood. This method is based on the idea that effects of plan forms, cross-section, hydraulic structures and bed variations appear in time series of water surface profiles observed during a flood. It has been shown that the numerical method using time series of observed water surface profiles applying the BVC method can elucidate flood flows and bed variations in short reach like a river mouth (Okamura 2013). However, the applicability of the BVC method to river fields with a complex river system like the lower Shinanogawa River has not been investigated enough.

The objectives of this study are to develop the numerical model applying the BVC method and 2D bed-variation analysis using time series of observed water surface profiles during the 2011 flood in the whole of the lower Shinanogawa River including the several river confluences and branches and to elucidate the flood propagation and bed variation in the complex river system. At last we clarify the propagation mechanism of the flood flow around river confluences, flood flow storages and bed variations in the lower Shinanogawa River by using the developed numerical model.

2 OBJECTIVE AREA AND FLOOD

Figure 1 shows the plan form of the lower Shinanogawa River and water-level observation points. No inflow enters from the Arai Weir located at the upstream end of the lower Shinanogawa River because the weir gates are completely closed during floods to prevent inflows of flood water from the upstream area. Therefore, the flood discharge hydrograph in the lower Shinanogawa River is almost determined by discharges from tributaries of the Ikarashigawa River and Kariyatagawa River. The discharge of the Nakanokuchigawa River is controlled by operating the Nakanokuchigawa Sluice Gate at the branch point of the Shinanogawa River and Nakanokuchigawa River.

Figure 2 is the enlarged figure of the dash box frame in Figure 1. As shown in Figure 2, no embankments are located at right bank of the reach from 47 km to 50.7 km and upstream of the inflow points of the Ikarashigawa River and Kariyatagawa River and the branch point of the Shinanogawa River and Nakanokuchigawa River. The area of the flood plain at no embankment

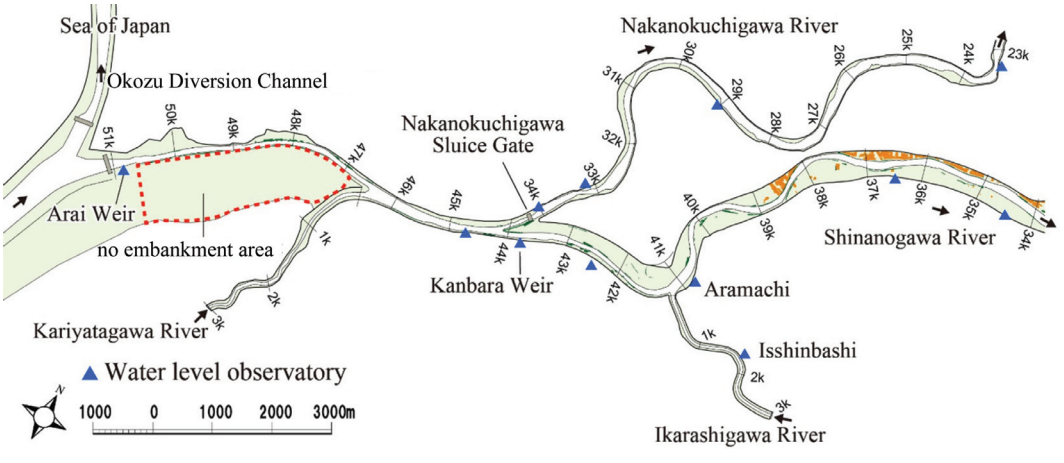

Figure 2. Plan form in the reach including the confluences of Ikarashigawa River and Kariyatagawa River and branch point of the Nakanokuchigawa River.

area is about 2.8 km^2 and the averaged elevation is about T.P. + 10.5 m. T.P. denotes Tokyo Peil, which is mean sea-level of Tokyo Bay.

Figure 3 shows the discharge hydrographs converted by H-Q curves at Aramachi located downstream of the confluence with the Ikarashigawa River, Teisekibashi located downstream of the confluence with the Nakanokuchigawa River, and the Nakanokuchigawa Sluice Gate. The figure shows that the discharge hydrographs with two peaks lasted for three days. The peak discharge almost reached the design flood discharge at Teisekibashi and Aramachi and exceeded the design flood discharge at the Nakanokuchigawa River.

Place	Teisekibashi	Aramachi	Nakanokuchigawa Sluice Gate
Discharge in 2011 flood (m^3/s)	3,402	2,528	520
Design flood discharge (m^3/s)	4,000	3,200	400

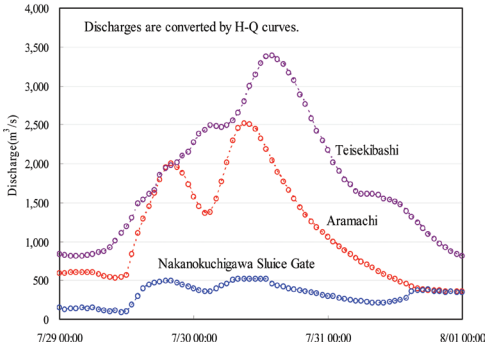

Figure 3. Discharge hydrographs converted by H-Q curves during the 2011 flood.

As shown in Figure 1, the Shinanogawa River and Nakanokuchigawa River flowing through the low-lying basin are equipped with many drainage pump stations and head works. Water levels have been recorded for operations. Therefore, we could get time series of observed water surface profiles at 1 to 5 km intervals by using water levels measured at the drainage pump stations and head works in addition to water-level gauging stations.

Figure 4 shows the time series of observed water surface profiles in the 2011 flood and longitudinal distributions of elevation on the levee crest and averaged bed elevation in the lower Shinanogawa River. Water levels at the peak discharge exceeded the High Water Level (H.W.L.) in the section located 26.0~42.0 km from the river mouth. Moreover, water levels exceeded flood plain elevations at the no embankment area and caused the vast inundation.

At the confluence of the Shinanogawa River and Ikarashigawa River indicated by dash box frame in Figure 4, adverse slopes of water surface profiles were seen because large inflows from the Ikarashigawa River caused backward flows. This fact shows that inflows from the Ikarashigawa River obviously had significant effects on the 2011 flood flow in the Shinanogawa River.

3 ANALYSIS OF FLOOD FLOWS AND BED VARIATIONS DURING THE 2011 FLOOD IN THE LOWER SHINANOGAWA RIVER

3.1 *Numerical analysis method*

We develop a numerical model applying unsteady flow and 2D bed-variation analyses using observed water-surface profiles in the lower Shinanogawa River. The numerical model consists of quasi-3D

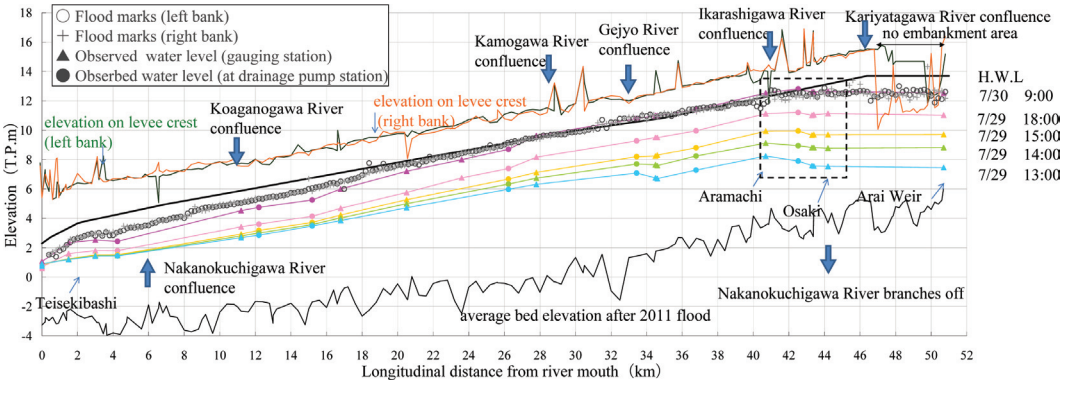

Figure 4. Time series of observed water surface profiles in the 2011 flood with the longitudinal distribution of elevation on the levee crest and averaged bed elevation in the lower Shinanogawa River.

unsteady flow analysis by the BVC method (Uchida and Fukuoka, 2012) and 2D bed-variation analysis.

The BVC method is able to evaluate vertical distributions of horizontal velocities and bottom velocities by introducing depth-averaged horizontal vorticity equation, horizontal momentum equation on water surface to shallow-water equation. A set of governing equations (1)~(5) is solved for the following unknown quantities: water depth h, Depth Averaged (DA) horizontal velocities U_i, DA horizontal vorticities Ω_i, horizontal velocities on water surface u_{si} and bottom velocities u_{bi} according to the process as shown in Figure 5. The bottom velocity is derived by integrating horizontal vorticities respect to depth (equation (1)).

$$u_{bi} = u_{si} - \Omega_j h \tag{1}$$

where, u_{bi}: bottom velocity, u_{si}: water surface velocity and Ω_j: DA horizontal vorticity.

To evaluate the bottom velocity by equation (1), BVC method is composed of depth-integrated horizontal vorticity equation (4) and water surface velocity equation (5) in addition to shallow water equations (2), (3). In this study, equation (2)~(5) are converted to the general curvilinear coordinate system.

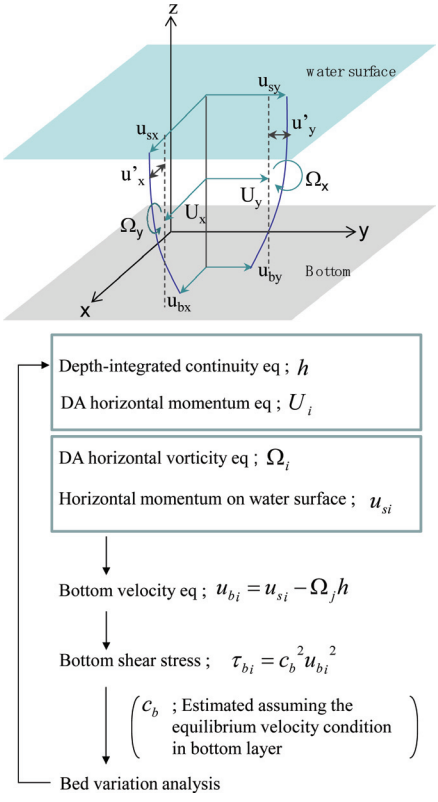

Figure 5. Flow of simulation method.

$$\frac{\partial h}{\partial t} + \frac{\partial U_j h}{\partial x_j} = 0 \tag{2}$$

$$\frac{\partial \rho U_i h}{\partial t} + \frac{\partial \rho U_i U_j h}{\partial x_j} = -\rho g h \frac{\partial z_s}{\partial x_i} - \tau_{0i} + \frac{\partial h\left(\tau_{ij} - \rho \overline{u'_i u'_j}\right)}{\partial x_j} \tag{3}$$

where, h: water depth, U_i: depth averaged horizontal velocity, ρ: density, g: gravity, z_s:water level, τ_0: bed shear stress, τ_{ij}: horizontal shear stress due to turbulence and $\overline{u'_i u'_j}$: correlation of vertical distributions of horizontal velocities u_i, u_j.

$$\frac{\partial \Omega_i h}{\partial t} = ER_{\sigma i} + P_{\omega i} + \frac{\partial h D_{\omega ij}}{\partial x_j} \tag{4}$$

where, ER: rotation term of vertical vorticity, $P_{\omega i}$: production term of vorticity from the bottom thin vortex layer and $D_{\omega ij}$: horizontal vorticity flux due to convection, rotation, dispersion and turbulence diffusion.

$$\frac{\partial u_{si}}{\partial t} + u_{sj}\frac{\partial u_{si}}{\partial x_i} = -g\frac{\partial z_s}{\partial x_i} + P_{si} \tag{5}$$

where, P_{si}: production term due to shear stress acting on thin water surface layer.

Vertical distributions of horizontal velocity are expressed by the cubic function (6) by using depth-averaged velocity U_i, velocity differences δu_i and Δu_i and dimensionless depth η, as;

$$u_i = U_i + \Delta u_i\left(12\eta^3 - 12\eta^2 + 1\right) - \delta u_i\left(4\eta^3 - 3\eta^2\right) \tag{6}$$

where,

$$\Delta u_i = u_{si} - U_i, \delta u_i = u_{si} - u_{bi}, \eta = \left(z_s - z_b\right)/h$$

The correlation of vertical distributions of horizontal velocities included in equation (3) is solved by equation (7) which is derived by integrating equation (6) respect to depth.

$$\overline{u'_i u'_j} = \frac{13}{35}\Delta u_i \Delta u_j + \frac{3}{35}\delta u_i \delta u_j - \frac{2}{35}\left(\Delta u_i \delta u_j + \Delta u_j \Delta u_i\right) \tag{7}$$

The bed variation is computed by the continuity equation for sediment and grain sizes (Hirano 1971) using bed load formula (Ashida and Michiue 1972) and suspended load formulas (Itakura and Kishi 1980; Lane and Kalinske 1941). The transport of the suspended sediment is computed by 2D advection and diffusion equations.

3.2 *Conditions of the numerical analysis*

We set the scope of the numerical model for the reach from the river mouth to the Arai Weir of the lower Shinanogawa River including the Nakanokuchigawa River, the Sekiya Diversion Channel and the confluences with the Ikarashigawa River, Kariyatagawa River, Gejyogawa River, Kamogawa River and Koaganogawa River. In addition, we included inundation areas due to no embankment in the scope of analysis, considering landforms of the flood plain using aerial laser profiler data.

The upstream boundary condition of the Shinanogawa River was given by no-flux condition because the Arai Weir gates at located around 51 km were completely closed during floods. The downstream boundary conditions of the Shinanogawa River and the Sekiya Flood Control Channel were given by the observed water level hydrographs at the river mouth.

Inflow discharge hydrographs from the several tributaries were provided so that the computed water-surface profiles in the whole of the Shinanogawa River agree with the observed ones.

The discharge hydrograph through the Nakanokuchigawa Sluice Gate was estimated so as to minimize the difference between observed and computed water-surface profiles in the upstream and downstream sections of the sluice gate by taking account of hydrostatic pressure and hydrodynamic pressure acting on the gate. Similarly, the discharge hydrograph through the Shinanogawa Sluice Gate was estimated by this method.

In the 2011 flood, a lot of waters in the river basin were pumped out by many drainage pump stations along the Shinanogawa River and Nakanokuchigawa River. Figure 6 shows temporal changes of observed total discharges from drainage pump stations in the Shinanogawa River and Nakanokuchigawa River. Maximum discharges in the Shinanogawa River and Nakanokuchigawa River were 480 m^3/s and 190 m^3/s, respectively and not negligible compared to the flood discharge. Therefore, observed discharge hydrographs from each pumping station were given for the analysis.

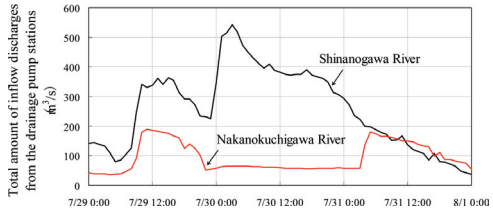

Figure 6. Temporal changes of observed total discharges from many drainage pump stations in the Shinanogawa River and Nakanokuchigawa River.

Figure 7 shows grain size distributions used for the analysis. The bed materials in the Shinanogawa River and Nakanokuchigawa River are composed of silt and sand and average diameters are about 0.5 mm.

The Manning roughness coefficients and vegetation permeability coefficients were determined so as to explain the time series of observed water-surface profiles in the 2011 flood by the BVC method. Manning roughness coefficients and vegetation permeability coefficients used in the analysis are shown in Table 1.

3.3 *Results and considerations*

3.3.1 *Water-surface profiles and flood discharge hydrographs in the lower Shinanogawa River*

Figure 8 shows the comparison between the computed and observed water-surface profiles and longitudinal distributions of the averaged bed elevations in the lower Shinanogawa River and Nakanokuchigawa River. In Figure 8(a), the computed water-surface profiles around the confluences of the several tributaries and branch point of the Nakanokuchigawa River could elucidate the observed ones in the Shinanogawa River. In addition, the computed water-surface profiles could explain the observed ones in the Nakanokuchigawa River (see Fig. 8(b)), while the computed water levels were lower than observed ones around directly downstream of the Nakanokuchigawa Sluice Gate. The water surface profiles at the peak time almost exactly matched flood marks in the Shinanogawa River and Nakanokuchigawa River.

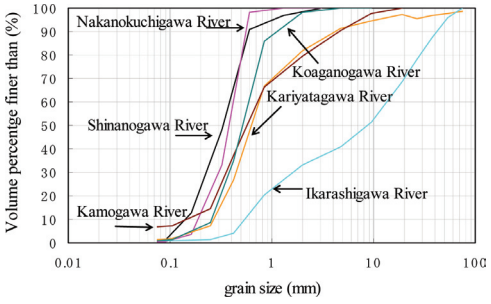

Figure 7. Grain size distributions used for the analysis.

Table 1. Manning roughness coefficient and vegetation permeability coefficient.

Section	Manning roughness coefficient ($m^{-1/3} \cdot s$)		Vegetation permeability coefficient (m/s)
	Main channel	Flood plain	
Sekiya flood control channel	0.013	0.030	–
Sinanogawa River (1.8~29 km)	0.020~0.028	0.025~0.040	40~90
Shinanogawa River (29~44 km)	0.028	0.025~0.050	20~90
Shinanogawa River (44~50.7 km)	0.025	0.030~0.050	40
Nakanokuchigawa River	0.022	0.030~0.050	20~90
Ikarashigawa River	0.027	0.035~0.055	–
Kariyatagawa River	0.025	0.030~0.040	–
Kamogawa River, Koaganogawa River, Gejyogawa River	0.020~0.030	0.030~0.070	–

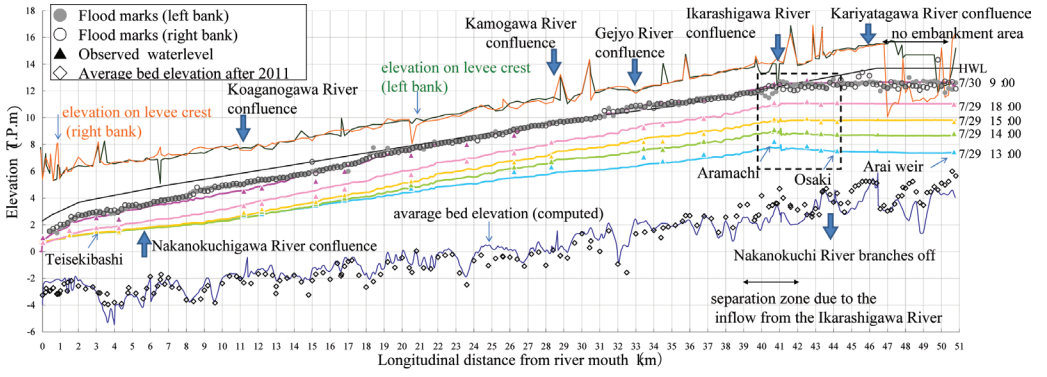

(a) Shinanogawa River

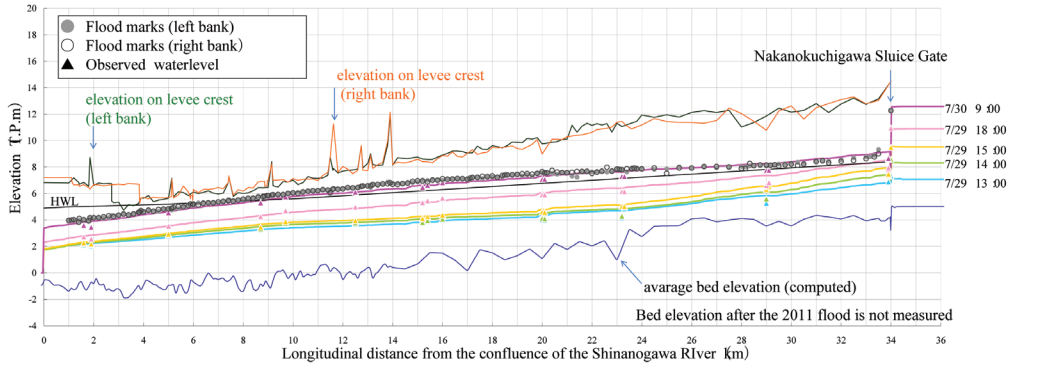

(b) Nakanokuchigawa River

Figure 8. Comparison between the computed and observed water-surface profiles and longitudinal distributions of the averaged bed elevations in the lower Shinanogawa River and Nakanokuchigawa River.

In Figure 8(a), the computed results almost agreed with observed average bed-elevations, while the bed elevations were estimated lower than the observations in the section located 39.0~42.0 km where a large separation area was formed due to large inflow rates from the Ikarashigawa River.

Figure 9 shows the discharge hydrographs and the temporal changes of the inundation volume at the no embankment area. Plots of the inundation volumes indicate values evaluated by using the observed water-level hydrograph at the Arai Weir and ground levels of the no embankment area. In

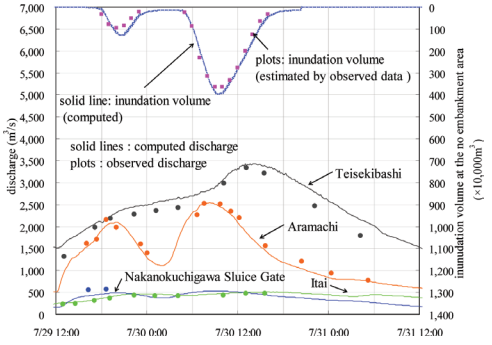

Figure 9. Discharge hydrographs and temporal changes of inundation volume at the no embankment area.

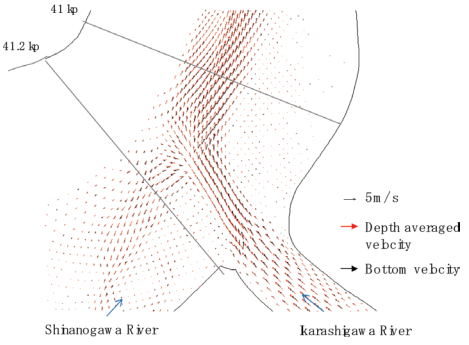

Figure 10. Computed horizontal velocity vectors at the peak of the first flood (18:00 on July 29).

this figure, we can see that the computed discharge hydrographs at Aramachi and Nakanokuchigawa Sluice Gate were in good agreement with the observed results. From our simulation, the inundation volume at the peak was estimated about 4,000,000 m^3. Although this is slightly higher than the estimated value, the computed results could estimate the storage and drainage of the inundation water in a flood period. The computed inundation volume hydrograph also coincided well with the estimated one.

3.3.2 *Flow and bed variation at the confluence of the Shinanogawa River and Ikarashigawa River*

Figures 10 and 11 shows the computed horizontal velocity vectors and bed variation contour at the peak of the first flood (18:00 on July 29) at the confluence of the Shinanogawa River and Ikarashigawa River. Here, red and black arrows in Figure 10 indicate the depth averaged velocity and bottom velocity respectively. Figure 12 shows computed discharge hydrographs in the section including the confluences of the Ikarashigawa River and Kariyatagawa River (see Fig. 2) with temporal changes of the inundation volume at the no embankment area.

The flow attacking point is seen at the left bank in 41.1 km point and the secondary flow is developed at the first peak as shown in Figure 10 since the inflow discharge from Ikarashigawa River is very large compared with that from the Shinanogawa River. Flow attacking to the river bank caused bank erosions as shown in Figure 11. The bed scouring occurred along the left bank of the main channel around 41 km point (see Fig. 11) where inflow discharges from the Ikarashi River concentrated. At the confluence of the Shinanogawa River and Ikarashigawa River indicated by dash box frame in Figure 8(a) the adverse

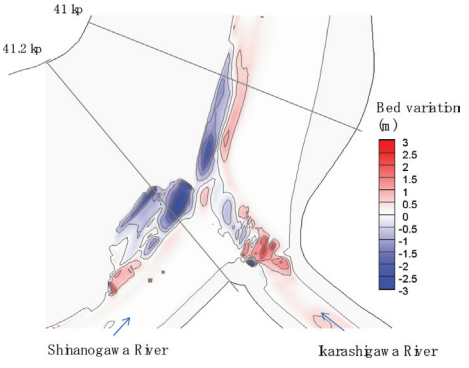

Figure 11. Computed bed variation contours at the peak of the first flood (18:00 on July 29).

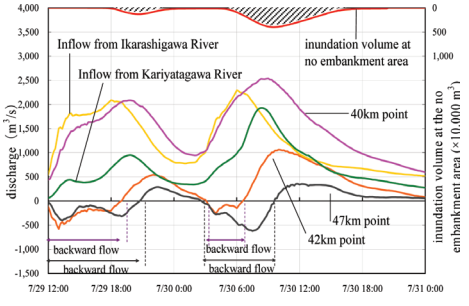

Figure 12. Computed discharge hydrographs in the section including the confluences of the Ikarashigawa River and Kariyatagawa River with temporal changes in inundation volume at the Nishino area.

slopes of water surface profiles are computed as well as the observed ones (see Fig. 4). The backward flow occurred at the confluence with the Ikarashigawa River and backward flow discharges reached to 580 m^3/s (see Fig. 12).

At the second flood, since inflow discharges from the Kariyatagawa River increased in addition to the inflow from the Ikarashigawa River, the inundation volume at the no embankment area increased and reached to maximum value during the flood. As above, the present numerical model could elucidate the flood flows and bed variation including large and small scale hydraulic phenomena in the lower Shinanogawa River with the complex river system.

4 CONCLUSION

In this study, we developed the numerical model consisting of the BVC method and 2D bed-variation analysis using observed water-surface profiles during the 2011 flood in the whole of the lower Shinanogawa River with the complex river system.

The present model explained well the observed discharge hydrographs and inundation volume hydrograph and averaged bed elevations in the whole of the lower Shinanogawa River during the flood. Furthermore secondary flow and bed variation at the confluence of the Shinanogawa River and Ikarashi River were described well, by this numerical model.

It was concluded that the present calculating method could elucidate the flood flows and bed variation including large and small scale hydraulic phenomena in the lower Shinanogawa River with the complex river system.

REFERENCES

Ashida, K. and Michiue, M. (1972). Study on hydraulic resistance and bed-load transport rate in alluvial streams. *Proc. JSCE, 206*, 59–69.

Engelund, F. (1974). Flow and bed topography in channel bends. *Journal of Hydraulics Division, Proc. of ASCE, Vol. 100, HY11,* 1631–1648.

Fukuoka, S. (2011). What is the fundamentals of river design—Utilization of visible techniques of sediment laden-flood flows. *Advances in River Engineering, JSCE, Vol. 17*, 83–88.

Fukuoka, S. and Uchida, T. (2013). Toward Integrated multi-scale simulations of flow and sediment transport in rivers. *Journal of Japan Society of Civil Engineers, Ser.B1 (Hydraulic Engineering), Vol. 69, No. 4*, II1–II10.

Hirano, M. (1971). River-bed degradation with armoring. *Proc. JSCE, 195*, 55–65.

Huang, J., Weber, L.J. and Lai, Y.G. (2002). Three-Dimensional Numerical Study of Flows in Open-Channel Junctions. *Journal of Hydraulic Engineering, ASCE, Vol. 128, No. 3*, 268–280.

Ishikawa, T., Suzuki, K. and Tanaka, M. (1986). Efficient numerical analysis of an open channel flow with secondary circulations, *Proc. of JSCE, Vol. 375/II-6,* 181–189.

Itakura, T. and Kishi, T. (1980). Open channel flow with suspended sediments. *Journal of Hydraulics Division, Proceedings of ASCE, Vol. 106, HY. 8*, 1325–1343.

Jin, Y.C. and Steffler, P.M. (1993). Predicting flow in curved open channels by depth-averaged method, *Journal of Hydraulic Engineering, ASCE, Vol. 119, No. 1,* 109–124.

Lane, E.W. and Kalinske, A.A. (1941). Engineering calculation of suspended sediment, *transactions of the American Geophysical Union, 20(3)*, 603–607.

Nishimoto, N., Shimizu, Y. and Aoki, K. (1992). Numerical simulation of bed variation considering the curvature of stream line in a meandering channel, *Journal of Japan Society of Civil Engineers, No. 456/II-21,* 11–20.

Okamura, S., Okabe, K. and Fukuoka, S. (2013). Bed variation analysis using the sediment transport formula considering the effect of river width and cross-sectional form in the Ishikari River mouth, *Floods From Risk to Opportunity, IAHS Publ. 357,* 217–224.

Uchida, T. and Fukuoka, S. (2011). Numerical Simulation of Bed Variation in a Channel with a Series of Submerged Groins, *Proceedings of the 34th IAHR World Congress,* 4292–4299.

Uchida, T. and Fukuoka, S. (2012). Bottom velocity computation method by depth integrated model without shallow water assumption, *Journal of JSCE, Ser.B1 (Hydraulic Engineering), Vol. 68, No. 4*, I1225–I1230.

Wu, W. (2008). Computational river dynamics, *Taylor & Francis, London*.